AIP | Applied Physics Letters

High refractive index composite for broadband antireflection in terahertz frequency range

Xuecheng Wang, Yunzhou Li, Bin Cai, and YiMing Zhu

Citation: Applied Physics Letters **106**, 231107 (2015); doi: 10.1063/1.4922574
View online: http://dx.doi.org/10.1063/1.4922574
View Table of Contents: http://scitation.aip.org/content/aip/journal/apl/106/23?ver=pdfcov
Published by the AIP Publishing

High refractive index composite for broadband antireflection in terahertz frequency range

Xuecheng Wang, Yunzhou Li, Bin Cai,[a] and YiMing Zhu[a]
Shanghai Key Lab of Modern Optical System and Engineering Research Center of Optical Instrument and System, Cooperative innovation centre of terahertz science, University of Shanghai for Science and Technology, Ministry of Education, Shanghai 200093, China

(Received 10 April 2015; accepted 4 June 2015; published online 11 June 2015)

In this study, titania–polymer composites with a very high refractive-index tenability and high transparency in the terahertz region were prepared. By controlling the blending ratio of the titania particle, a broad refractive-index tuning range from 1.5 to 3.1 was realized. Then, the composites were used to fabricate antireflective (AR) layers of high-resistivity silicon (HR-Si). By utilizing the thermoplasticity of the titania–polymer composite, a graded-index structure was fabricated via a hot-embossing method. Because of the good refractive-index matching between the composite and the HR-Si substrate, a broadband (0.2–1.6 THz, 7% reflection) AR layer was fabricated. © *2015 AIP Publishing LLC*. [http://dx.doi.org/10.1063/1.4922574]

The terahertz (THz) frequency range is broadly defined from 0.1 to 10 THz and is sandwiched between the microwave and mid-infrared frequency ranges.[1] On account of its potential application in molecular biological science, medical imaging, astronomy, and future communication systems,[2–4] considerable efforts have been carried out worldwide over the past decades.[5–7] However, THz components such as THz sources, modulators, and detectors still suffer various problems. Among them, one of the biggest problems is surface reflection loss. To improve system performances, it is very important to reduce the surface reflection.

Conventional antireflective (AR) coatings consisting of monolayer or multilayered systems are based on the interference between the incident and reflected light. In this way, the AR coating is usually a quarter-wave thin film, which has a refractive index of $n = n_{substrate}^{1/2}$. This type of homogeneous AR coating can achieve low reflection, but it is restricted owing to its inadaptability for broadband antireflection applications and the difficulty of finding proper materials. Another approach for achieving the broadband antireflection effect is the use of subwavelength surface-relief structures. Along with the changes in the surface structures, the effective refractive index is gradually changed; consequently, minimized Fresnel reflection can be realized. Arrays have been proposed to realize these graded-index surface structures consisting of nanotips,[8] micropyramids,[9] and micro-semisphere[10] arrays were proposed, which yielded a minimum reflectance of 25%, 3%, and 1.8%, respectively, over broad THz ranges. Although those structures show excellent antireflective effects, they suffer disadvantages such as the complicated fabrication steps or substrate limitation.[11–13] For example, the isotropic wet etching technique of pyramid structure is limited on crystalline silicon substrate. On the other hand, polymers are versatile materials that have an excellent processability and are light, low-cost, and very transparent in the THz region for some non-polarized species. Many optical polymers such as polyethylene (PE), polymethylpentene (TPX), and cyclo-olefin polymer (COP) show relatively low optical loss across the THz regime, and have found many usages as lenses, windows, and waveguide.[14,15] By utilizing the thermoplasticity of polymers, a surface relief structure can be easily fabricated; However, the performance of these polymers was limited by their low refractive indices. Thus, flexible and transparent materials with a wide tunable range of the refractive index, which is vital for refractive-index matching, are crucial for THz optics.

In this study, an optical COP was hybridized with high-refractive-index titania particles, and a series of transparent high-refractive-index inorganic–organic composites was prepared. Then, the composite with the highest refractive index of 3.1 was applied to fabricate an AR coating on silicon substrates. Utilizing the thermoplasticity of the composite, a subwavelength surface-relief structure pattern was fabricated by a hot-embossing technique via a handmade metallic mold. By this simple process, an outside-in gradual effective refractive-index profile for antireflection was constructed on a silicon wafer surface. The optical characteristics of the surface-modified silicon in the THz range were investigated using THz time-domain spectroscopy (THz-TDS). Compared with a low-refractive-index polymer, the composite exhibited an obvious advantage for AR applications, and a significant broadband AR effect (0.2–1.6 THz, 7%) was achieved.

In our experiment, a low-loss COP with a frequency-independent refractive index of 1.52 was used for preparation of the organic–inorganic composite. The COP is also resistive to most acids and water, making it a good choice as a substrate material for broadband THz spectroscopy. In order to increase the refractive index of the polymer, titania nanoparticles with a rutile crystal structure are a good additive because of the relatively low optical loss and very high permittivity at THz frequency.[16] Owing to the long-wavelength nature of THz radiation, the optical performance of the composites in this wavelength regime is much less affected by scattering from particle aggregation (one or two

[a]Authors to whom correspondence should be addressed. Electronic addresses: bullcai@gmail.com and ymzhu@usst.edu.cn

orders of magnitude smaller than the THz wavelength). According to Rayleigh scattering theory, the scattering losses can be neglected for a particle size less than 10 μm. Therefore, titania particles with a diameter of 1 μm were used to prepare the TiO_2-COP composites. First, in order to suppress the aggregation of the particles, we utilized a bead-milling method[17] to disperse and modify the surfaces of the TiO_2 microparticles (1 μm diameter) in a toluene solvent. Then, the COP polymer was dissolved in the TiO_2 suspensions and mixed by stirring at 300 rpm for approximately 5–8 h. The homogenized TiO_2-COP mixture was casted on glass substrate and baked in a vacuum oven at 60–80 °C for approximate 6–8 h. The fully dried TiO_2-COP composites can be easily peeled from the glass substrate and prepared for THz-TDS. We obtained transmission measurements of the fabricated TiO_2-doped and undoped COP films using a THz-TDS system (FiCO, @Zomega Corp.). From the Fig. 1, we can see that the refractive index increased dramatically as the TiO_2 doping ratio increased. We obtained the refractive indices of 1.73, 1.98, and 3.10 by the weight ratio of 30 wt. %, 50 wt. %, and 80 wt. %, respectively. Furthermore, the refractive indices of the composites remained practically constant throughout the 0.1–1.6 THz range [inset of Fig. 1]; this property is beneficial for broadband THz device fabrication.

The refractive index of the TiO_2-COP composite was modeled with Bruggeman's effective medium approximation[18]

$$1 - f_v = \frac{\varepsilon_{particle} - \varepsilon_{composite}}{\varepsilon_{particle} - \varepsilon_{cop}} \sqrt[3]{\frac{\varepsilon_{cop}}{\varepsilon_{composite}}}, \quad (1)$$

where $\varepsilon_{particle}$, ε_{cop}, and $\varepsilon_{composite}$ denote the permittivities of the dielectric particles, COP, and composite, respectively; and f_v is the volumetric particle fraction ($0 < f_v < 1$) of the particles used for doping. The volumetric fraction of TiO_2 particles can be calculated by the equation: $f_v = f_\omega / [f_\omega + (1 - f_\omega)\rho_{particle}/\rho_{cop}]$, where f_ω is the particles weight fraction, $\rho_{particle}$ and ρ_{cop} are the densities of particles and host polymer, respectively. In our experiment, ε_{cop} of the pure host COP is 2.310 ($n_{cop} = 1.52$), $\varepsilon_{particle}$ of rutile TiO_2 is 39.5, ρ_{cop} of the COP is 0.950 g/cm^3 (ZEONEX 480 R), and $\rho_{particle}$ of rutile TiO_2 is 4.274 g/cm^3 (YFNANO: YFO04-U1). From the data fitting, we can see that the Bruggeman model is in good quantitative agreement with experimentally measured refractive indices (Fig. 1, solid line).

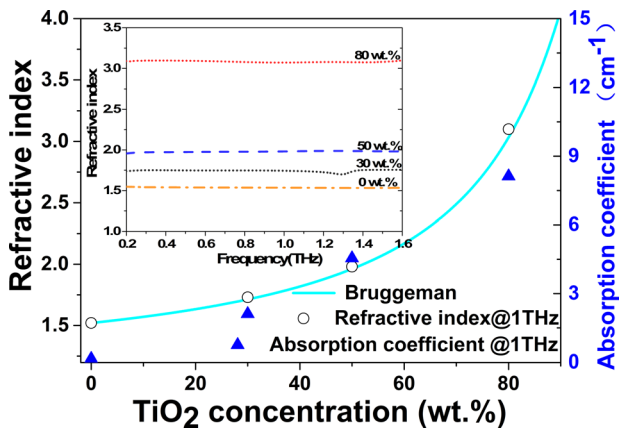

FIG. 1. Changes in the refractive index and absorption coefficient of the TiO_2-COP composites as a function of the TiO_2 doping ratio. The experimental data were fitted by the Bruggeman model (solid line). Inset: the refractive indices of pure COP (2-mm-thick) and TiO_2-COP composites of 30 wt. %(254-μm-thick), 50 wt. % (256-μm-thick) and 80 wt. % (253-μm-thick) TiO_2 doping ratio, respectively.

From the experiments, we observed that the transmittances of the composites decrease when the particle concentrations increase, as shown in Fig. 2. The high refractive index of the composites plays a negative role in the transmittance decreasing; that is, the Fresnel reflections were too high to be neglected. Fig. 2 shows the results after compensation for Fresnel reflection. The film exhibits considerable transparency in the THz region. Moreover, the transmittance of samples decreased as the frequency increased; this could be due to the absorption and scattering of the TiO_2 particles (Fig. 1).

In THz systems, high-resistivity silicon (HR-Si) is a suitable material for a wide range of THz components owing to its broadband transparency and low dispersion.[19,20] However, silicon is usually associated with a high Fresnel reflection loss (approximately 30% in power from a single surface) because of its high dielectric constant. To improve system performance, it is of great importance to reduce the reflection at the air–silicon interface to increase the dynamic range and improve the spectral resolution. For silicon optics in the THz spectral region, a plastic layer of parylene and polyethylene was developed.[21,22] However, these materials only have a refractive index of 1.62 and 1.5 in the THz spectral range, which is lower than the theoretical requirement ($n = n_{substrate}^{1/2} = 1.85$). Other antireflection techniques such as a multilevel AR coating, a coating consisting of thin metallic layers, and a subwavelength surface-relief structure on a silicon substrate have been developed.[23,24] However, the fabrication procedures are usually complex, and suitable optical materials for matching the refractive index of the substrate are inadequate.

In this experiment, as one of the applications of the TiO_2-COP composite, we utilized the fabricated composite to create an AR layer on a silicon substrate (resistivity > 10 000 Ω·cm) by a hot-embossing technique. To match the refractive-index gap between air and silicon, an 80 wt. % TiO_2-COP composite ($n = 3.10$) was employed for fabrication of the AR coating. First, an 80 wt. % TiO_2-COP composite was cast onto a

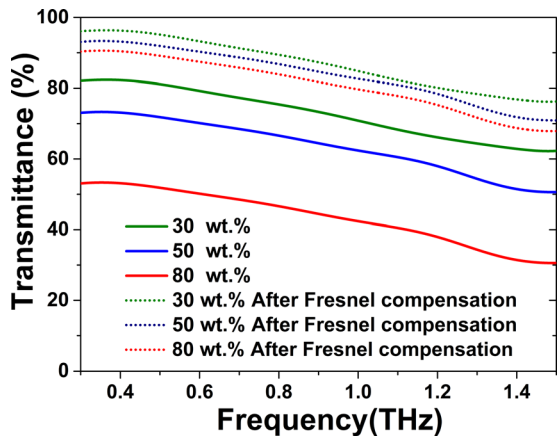

FIG. 2. Transmittance of the polymer composite as function of the weight ratio of TiO_2 doping, and the data after compensation for Fresnel reflection.

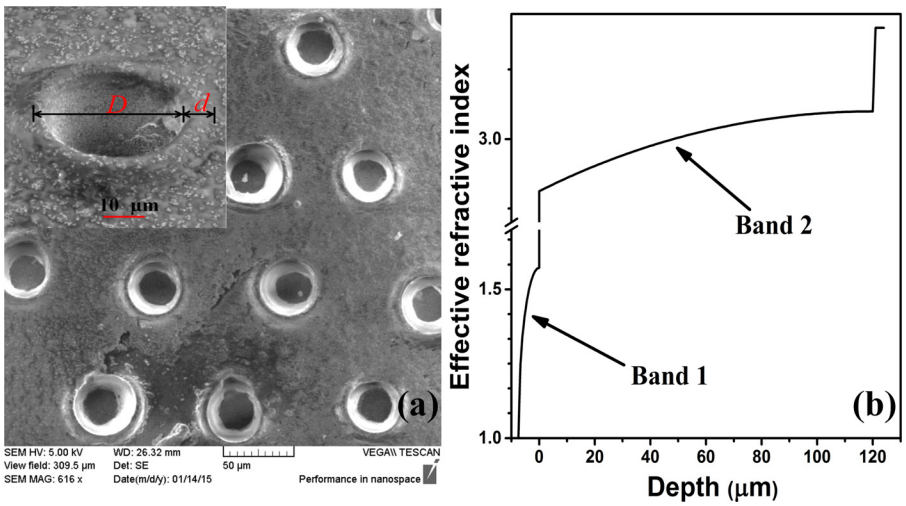

FIG. 3. (a) SEM image of the AR structure obtained by the hot-embossing process. (b) The effective refractive-index profile of the AR structure.

silicon substrate; then, the substrate was placed onto a hot plate to maintain a constant temperature in the range of 50–60 °C for approximately 3 h to remove the solvent. Next, the composite-coated HR-Si sample and a handmade metallic mold were heated to 180 °C, and a metallic mold was then pressed into the composite layer to deform the composite layer. Finally, after cooling the system, the metallic mold was separated from the composite layer. A scanning electron microscopy (SEM) image of the deformed layer is shown in Fig. 3(a). We see that the composite layer was transformed into an array of holes with hole diameters (D) in the range of 35–45 μm [Fig. 3(a), inset]. The holes were surrounded with annular bulges having a width (d, difference between the inner and outer diameters) of 10–20 μm. These annular bulges are the result of the extrusion from needle tips. The microstructured TiO_2-COP composite AR layer can be considered as a series of thin layers with continuously changing filling factors. The effective refractive index (n_{eff}) of each layer can be expressed by[9,25]

$$n_{eff} = \sqrt{n_{air}^2 \times S_{air}\% + n_{composite}^2 \times S_{composite}\%}, \qquad (2)$$

where n_{air} is the refractive index of air, $S_{air}\%$ is the areal fraction occupied by air, $n_{composite}$ is the refractive index of the TiO_2-COP composite, and $S_{composite}\%$ $(1 - S_{air}\%)$ is the areal fraction occupied by the TiO_2-COP composite. Using Eq. (2), the refractive-index profile of the microstructured TiO_2-COP composite layer can be roughly calculated, as shown in Fig. 3(b). We obtained two gradually changing index profiles. Band 1, from 1.0 to 1.6 (from −8 to 0 μm), is ascribed to the annular bulges, and Band 2, from 1.6 to 3.1 (0–120 μm), is ascribed to the reverse cone structure. To evaluate the performance of the embossed AR structures, a quarter-wave layer for a specific wavelength was also investigated as one of the comparative targets. For THz waves with a center frequency of 0.5 THz, the corresponding quarter-wavelength is approximately 120 μm.

The AR effect of the samples was investigated by THz-TDS, and the results are shown in Fig. 4 (the reflection peaks in the time-domain spectra, which originate from the Fabry–Perot effect, were cut off to make the experimental results smooth). The black dotted line is the transmitted intensity of a bare HR-Si substrate. The red dotted line represents the transmittance of a single TiO_2-COP layer (1/4 λ thickness, $n = 1.73$) coated silicon substrate, which has two enhanced peaks that appear at 0.50 THz (71%) and 1.45 THz (61%) (in Fig. 4), respectively. Furthermore, we also fabricated a single AR-coated (1/4 λ thickness) silicon substrate by using polystyrene (PS) (pink dotted line). The single TiO_2-COP layer exhibits higher performance than the single PS layer in the ranges of 0.2–0.86 THz and 1.25–1.6 THz. This is mainly attributed to the better refractive-index matching between silicon and the AR layer. However, there is one region around 1.02 THz where the TiO_2-COP quarter-wave-coating sample has a transmittance of 45.3%, which is lower than that of the silicon substrate. This could be due to the absorption of the composite layer.

The single-side embossed PS layer exhibits an enhanced transmittance compared to the single-PS-layer sample throughout the frequency range from 0.2 to 1.5 THz. The single-side embossed TiO_2-COP layer sample exhibited the best overall AR properties compared to the other samples, and an average transmittance of up to 64% throughout the frequency range from 0.2 to 1.6 THz was achieved. Here, it must be noted that the sample suffered from an additional Fresnel loss of approximately 28% during the measurement

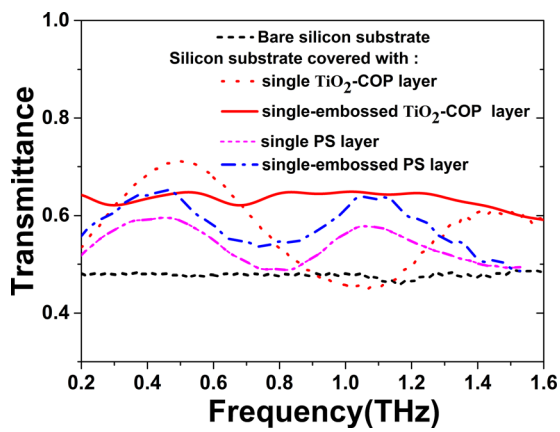

FIG. 4. Transmittance spectra of the bare HR-Si substrate and an HR-Si substrate covered with a single layer of TiO_2-COP, a single layer of PS, a single-side embossed PS layer, and a single-side embossed TiO_2-COP composite layer.

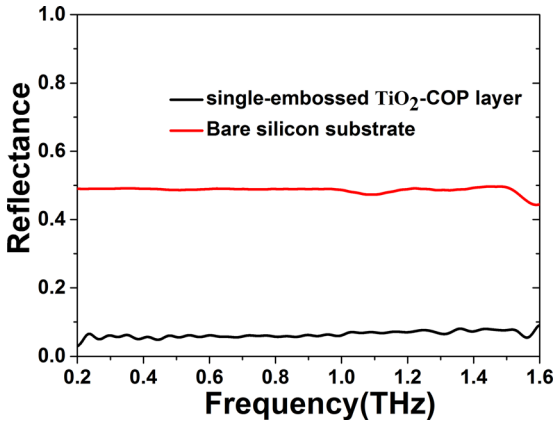

FIG. 5. Reflectance spectra of the bare HR-Si substrate and an HR-Si substrate covered with a single-side hot-embossed TiO_2-COP AR layer.

because of rear-side (noncoating) reflection. The AR effect of the single-side embossed TiO_2-COP layer originates from two mechanisms. One is due to the two graded indices changing bands, and the other one could be attributed to the multilayered coating. In the second case, Band 1 can be equivalently thought of as a low-refractive-index layer, whereas Band 2 can be thought of as a high-refractive-index layer.

We also investigated the reflectance of a structured TiO_2-COP sample by THz-TDS. From Fig. 5, the reflectivity of such an outside-in gradual refractive-index structure was approximately 7%. The results demonstrate that the graded-index coating yields broadband antireflection characteristics.

In summary, TiO_2-COP composites for THz applications were prepared; the composites not only exhibit good transparency in the range of 0.1–1.6 THz but also have a very large refractive-index tunability from 1.5 to 3.1. By utilizing thermal deformation properties, the TiO_2-COP composite was applied to an HR-Si substrate for broadband antireflection structures via a hot-embossing process. Although the embossed structure needs to be further optimized, the proposed structure provides a far broader bandwidth for the AR effect (0.2–1.6 THz, 7% reflection) than the homogeneous AR layer. This kind of inorganic–organic composites are highly transparent, refractive-index tunable, and thermally deformable and can be broadly applied to the fabrication of AR coatings, waveguides, photonic crystals, etc., for controlling and manipulating THz radiation.

This work was partly supported by the National Program of Key Basic Research Project of China (973 Program, 2014CB339806), Major National Development Project of Scientific Instrument and Equipment (Nos. 2011YQ150021 and 2012YQ14000504), National Natural Science Foundation of China (Nos. 61138001, 61205094, 61307126, and 1377111), Key Scientific and Technological Project of Science and Technology Commission of Shanghai Municipality (Nos. 12142200100, 12JC1407100, 14DZ1206600, and 1323120310), Program of Shanghai Subject Chief Scientist (14XD1403000), New Century Excellent Talents from Ministry of Education (NCET-12-1052), Scientific Research Innovation Project of Shanghai Municipal Education Commission (No. 12510502300).

[1]B. Ferguson and X.-C. Zhang, Nature Mater. **1**, 26 (2002).
[2]B. M. Fischer, M. Hoffmann, and H. Helm, Opt. Express **13**, 5205 (2005).
[3]M. Tonouchi, Nat. Photon. **1**, 97 (2007).
[4]R. Kakimi, M. Fujita, M. Nagai, M. Ashida, and T. Nagatsuma, Nat. Photonics **8**(8), 657–663 (2014).
[5]T. Matsui, A. Agrawal, A. Nahata, and Z. V. Vardeny, Nature **446**, 517 (2007).
[6]A. L. Bingham and D. Grischkowsky, Appl. Phys. Lett. **90**, 091105 (2007).
[7]M. Skorobogatiy and A. Dupuis, Appl. Phys. Lett. **90**, 113514 (2007).
[8]Y. F. Huang and S. Chattopadhyay, J. Nanophotonics **7**(1), 073594 (2013).
[9]Y. W. Chen, P. Y. Han, and X.-C. Zhang, Appl. Phys. Lett. **94**, 041106 (2009).
[10]D. S. Kim, D. J. Kim, D. H. Kim, S. Hwang, and J. H. Jang, Opt. Lett. **37**(13), 2742–2744 (2012).
[11]C. H. Sun, P. Jiang, and B. Jiang, Appl. Phys. Lett. **92**, 061112 (2008).
[12]D. S. Kim, M. S. Park, and J. H. Jang, J. Vac. Technol. B **29**, 020602 (2011).
[13]C. Brückner, B. Pradarutti, O. Stenzel, R. Steinkopf, S. Riehemann, G. Notni, and A. Tünnermann, Opt. Express **15**, 779 (2007).
[14]R. Mendis and D. Grischkowsky, J. Appl. Phys. **88**, 4449 (2000).
[15]K. Nielsen, H. K. Rasmussen, A. J. L. Adam, P. C. M. Planken, O. Bang, and P. U. Jepsen, Opt. Express **17**, 8592 (2009).
[16]P. H. Bolivar, M. Brucherseifer, J. G. Rivas, R. Gonzalo, I. Ederra, A. L. Reynolds, M. Holker, and P. De Maagt, IEEE Trans. Microwave Theory Tech. **51**, 1062 (2003).
[17]B. Cai, O. Sugihara, H. I. Elim, T. Adschiri, and T. Kaino, Appl. Phys. Express **4**(9), 092601 (2011).
[18]M. Scheller, S. Wietzke, C. Jansen, and M. Koch, J. Phys. D: Appl. Phys.**42**, 065415 (2009).
[19]K. Y. Kim, A. J. Taylor, J. H. Glownia, and G. Rodriguez, Nat. Photonics **2**, 605 (2008).
[20]X. Wu, X. Pan, B. Quan, and L. Wang, Appl. Phys. Lett. **103**(12), 121112-1–121112-5 (2013).
[21]A. J. Gatesman, J. Waldman, M. Ji, C. Musante, and S. Yngvesson, Microwave Guided Wave Lett. **10**, 264–266 (2000).
[22]W. Withayachumnankul, B. M. Fischer, S. P. Mickan, and D. Abbott, Microwave Opt. Technol. Lett. **49**, 2267–2270 (2007).
[23]H. T. Chen, J. Zhou, J. F. O'Hara, F. Chen, A. K. Azad, and A. J. Taylor, Phys. Rev. Lett. **105**, 073901 (2010).
[24]W. E. Lai, H. W. Zhang, Y. H. Zhu, Q. Y. Wen, W. W. Du, and X. L. Tang, Opt. Express **22**(3), 2174 (2014).
[25]L. Escoubas, J. J. Simon, M. Loli, G. Berginc, F. Flory, and H. Giovanni, Opt. Commun. **226**, 81 (2003).